Evaluation of the Fit of CAD/CAM Abutments

Adam Hamilton, BDSc, FRACDS, DCD[a]/Roy B. Judge, BDS, LDS, RCS, MDSc, PhD[b]/
Joseph E. Palamara, BDSc, Dip Ed, PhD[c]/Christopher Evans, BDSc (Hons), MDSc, MRACDS[d]

Purpose: This study aimed to compare the fit of computer-aided design/computer-assisted manufacture (CAD/CAM) abutments provided by a single system with proprietary prefabricated abutments on various implant systems. ***Materials and Methods:*** Titanium CAD/CAM abutments were compared with prefabricated abutments on five different implant types. The samples were embedded in epoxy resin, sectioned longitudinally, and polished. Scanning electron microscopy was used to measure the gap between the implants and abutments at the connecting flanges and internal features. Independent *t* tests were used to compare data. ***Results:*** A mean difference of 1.86 μm between the gold synOcta and CAD/CAM abutments on the Straumann Standard Plus implant was observed to be statistically significant ($P = .002$). Less than 0.4 μm of difference was found between the CAD/CAM and prefabricated abutments for the remaining implant types, and statistical significance was not observed. Mean differences of 34.4 μm (gold) and 44.7 μm (titanium) were observed between the CAD/CAM and prefabricated abutments on the Straumann Standard Plus implants, which were statistically significant ($P < .001$). A mean difference of 15 μm was also observed between the CAD/CAM and prefabricated abutment on the NobelReplace implant, which was statistically significant ($P = .026$). All other groups had less that 4 μm of difference, and statistical significance was not observed. ***Conclusion:*** The CAD/CAM abutments appeared to have a comparable fit with prefabricated abutments for most of the systems evaluated. Design differences between the abutment connections for both Straumann implants were observed that affected the fit of internal components of the implant-abutment connections. *Int J Prosthodont 2013;26:370–380. doi: 10.11607/ijp.3501*

An important aspect of an implant abutment is the mating surface that forms part of the implant-abutment connection. The design of the fitting surface and mode of abutment manufacturing will influence the precision of fit between the implant and abutment. Several issues have been reported with abutment misfit and microgaps, including screw loosening,[1–3] micro/bacterial/molecular leakage,[4–10] abrasion and wear of components,[11] potential for bone loss,[12,13] and the "micropump effect."[14,15]

Computer-aided design/computer-assisted manufacture (CAD/CAM) systems are currently available that are capable of manufacturing prosthetic abutments across multiple dental implant systems and connection designs. However, there is little published research regarding the fit of CAD/CAM abutments to implants manufactured using these commercially available systems.[16]

There have been literature reviews focusing on the assessment of the fit of implant prostheses; however, they only assessed partial denture frameworks splinting multiple implants.[17] Literature pertaining to the assessment of fit for single implant restorations is limited, and a standardized methodology has not yet been established. The implant-abutment connection for unsplinted restorations is subjected to considerably more stress and bending moments during nonaxial loading, making precision of fit much more critical.[18,19]

Previous studies have assessed the implant-abutment fit using various methodologies, including direct measurement of implant components, marginal adaptation, internal adaptation evaluated following sectioning, radiographic appearance, microleakage, and the degree of rotational freedom.[8,20–25]

[a]Private Practice, Perth, Australia.
[b]Associate Professor and Head of Prosthodontics, Melbourne Dental School, University of Melbourne, Melbourne, Australia.
[c]Associate Professor, Melbourne Dental School, University of Melbourne, Melbourne, Australia.
[d]Private Practice and ITI Fellow, Melbourne, Australia.

Correspondence to: *Dr Roy Judge, 5th Floor, 720 Swanston Street, Carlton 3053, Victoria, Australia. Fax: +613 9341 1595. Email: roybj@unimelb.edu.au*

Table 1 Implant-Abutment Configuration Details

Implant type	Interface and connection type	Group	Abutment type	Recommended torque (Ncm)
Bränemark System RP	Butt joint with external hexagon	1 (BE)	Esthetic	35*
		2 (BP)	NobelProcera CAD/CAM titanium	35*
NobelReplace RP	Butt joint with internal tri-channel and cam tube	3 (RE)	Esthetic	35*
		4 (RP)	NobelProcera CAD/CAM titanium	35*
Astra Tech OsseoSpeed 4.0	11-deg internal conical taper with internal hexagon	5 (AT)	TiDesign 3.5/4.0	20*
		6 (AP)	NobelProcera CAD/CAM titanium	20*
Straumann Bone Level RC	15-deg internal conical taper with internal cross fit connection	7 (SblA)	RC anatomical	35*
		8 (SblP)	NobelProcera CAD/CAM titanium	35*
Straumann Standard Plus RN	45-deg external bevel with 8-deg internal conical taper and internal octagon	9 (SG)	RN synOcta gold	35*
		10 (SM)	RN synOcta RN synOcta titanium meso milling cylinder	35* 15†
		11 (SP)	NobelProcera CAD/CAM titanium	35*

*Torque used for abutment screw.
†Torque used for prosthetic screw.

To justify their use, CAD/CAM abutments should be able to produce a degree of fit comparable with proprietary prefabricated abutments produced by each individual implant manufacturer. The purpose of this study was to assess and compare the fit of prefabricated abutments with abutments manufactured by a CAD/CAM system.

Materials and Methods

The 11 implant-abutment configurations evaluated in this study are listed in Table 1. Each implant, its prefabricated abutment, and screw were obtained from their respective manufacturers. NobelProcera CAD/CAM abutments (Nobel Biocare) were also acquired for each of the five implant types. The intentional use of the components for research was not disclosed to the manufactures.

A one-piece abutment was evaluated for each of the implant types with the exception of the titanium prefabricated abutments for the Straumann Standard Plus implants (Straumann). Two prefabricated abutment configurations were evaluated separately for this implant: a one-piece gold synOcta abutment (Straumann) and a titanium synOcta abutment (Straumann) used in conjunction with a synOcta Titanium Meso Milling Cylinder (Straumann).

Digital scanning electron microscopy (SEM) (Quanta Model 200, FEI) images were taken of the fitting surfaces of a representative number of samples for observational assessment under low vacuum in secondary electron mode. Each implant-abutment configuration was then assembled with screws tightened to their recommended torque, as listed in Table 1, using a manual torque wrench (Nobel Biocare). The sample was then placed at the base of a 40-mm cylindrical reusable plastic mold former (FixiForm, Struers) and visually aligned such that its long axis was parallel to the mold base and held in position using a plastic clip (Multiclips, Struers). The axial rotation of the implant was also controlled such that the plane of grinding was perpendicular to the flat opposing antirotation features of the implant-abutment connection, which was marked with a graphite pencil on the exterior of the implant prior to assembly of the components. The specimens were then cold mounted with epoxy resin (Epofix, Struers) and placed under vacuum for 10 minutes to remove any air bubbles. The specimens were then allowed to cure for at least 24 hours at room temperature.

Using a non-fixed sample holder, six specimens were then ground and polished concurrently in an automated lapping machine (Tegrapol-25, Struers) that had controlled force application, control of rotational speed/direction of both the grinding and polishing disk as well as the specimen holder, and automated lubricant/water dosing.

Following the regime recommended for metallographic polishing of titanium,[26–28] grinding of the specimens was accomplished with 120-grit silicon carbide foil, followed by 600-grit silicon carbide foil (Struers) at 300 rpm and 10 N of force on each

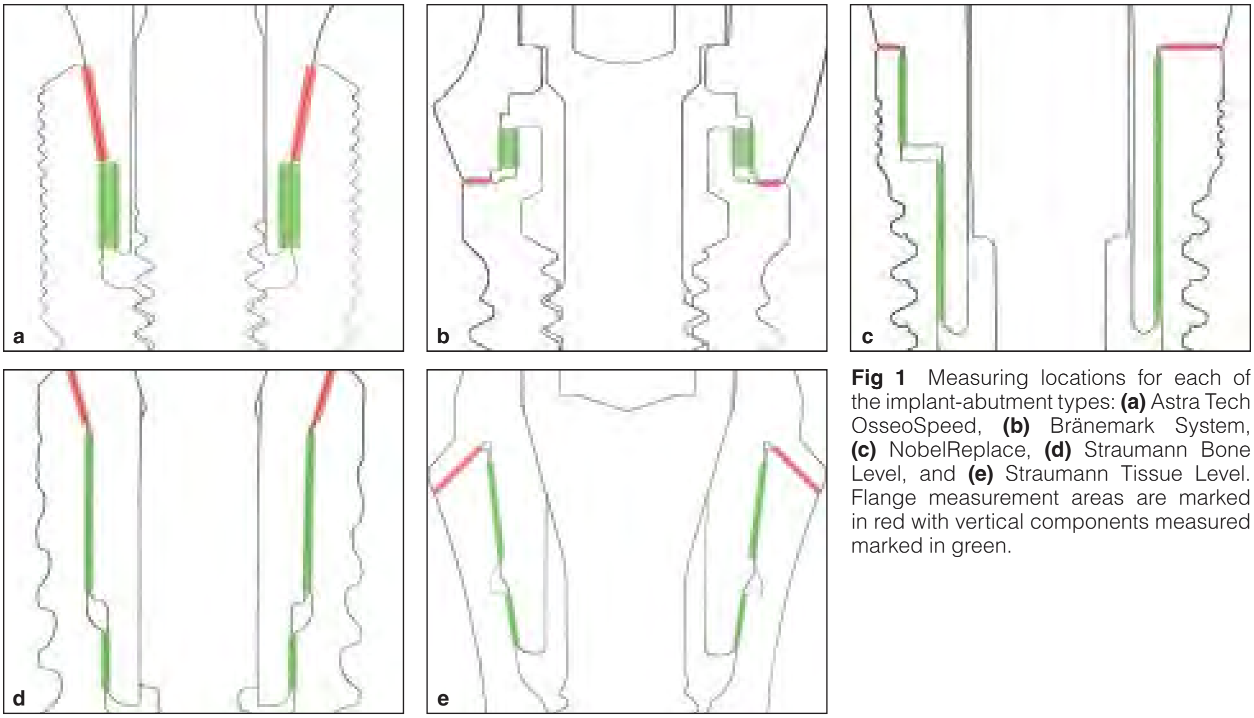

Fig 1 Measuring locations for each of the implant-abutment types: **(a)** Astra Tech OsseoSpeed, **(b)** Brånemark System, **(c)** NobelReplace, **(d)** Straumann Bone Level, and **(e)** Straumann Tissue Level. Flange measurement areas are marked in red with vertical components measured marked in green.

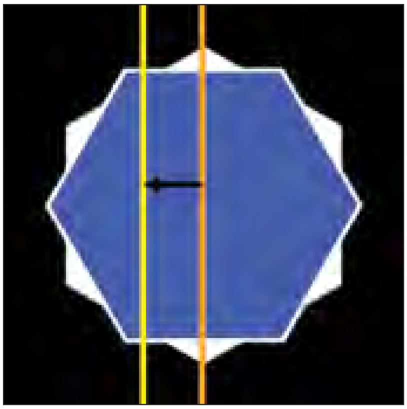

Fig 2 Double hex configuration within vertical components of samples BE, AT, and AP. Orange line depicts midpoint reached during initial grinding and polishing where flange components were measured. Yellow line depicts second plane of grinding and polishing where measurements were made for the vertical components of the connection.

specimen in a complimentary direction with continuous water flow until the center of the specimen was reached. Initial polishing was performed with 9-μm diamond polishing paste (Diapro Allegro/Largo, Struers) on a composite polishing disk (MD-Largo, Struers) for 5 minutes. A final polish was performed with colloidal silica (OP-S suspension, Struers) and 30% hydrogen peroxide mixed in a ratio of 9:1 on a porous neoprene cloth (MD-Chem, Struers) for 7 minutes. Both polishing stages were performed at 150 rpm with 10 N of force on each specimen with a complimentary direction used for the diamond polishing and counter-rotation used for the final polishing with the colloidal silica. A thorough washing was performed with water and ethanol after each stage of grinding and polishing.

Prior to grinding and polishing, the underside of the specimen was ground parallel to the base of the specimen with which the implant was aligned to ensure viewing from a perpendicular angle when placed on the SEM stage.

Each of the specimens was assessed following polishing to determine whether any deformation of the surface was present. Viewing of the specimens with reflected light microscopy and polarized light filters enabled the grain structure to be clearly visualized without etching of the titanium surface, provided a relatively deformation-free surface was achieved.[27] If the grain boundaries were not clearly visible, this indicated that some deformation on the surface specimens was still present and polishing procedures were repeated.

Table 2 Statistical Analysis of Comparison Between Prefabricated and CAD/CAM Abutments

		Flange data					Vertical data				
Implant	Abutment	Mean microgap (µm)	SD	Difference (compared to CAD/CAM)	*P*	95% CI	Mean gap (µm)	SD	Difference (compared to CAD/CAM)	*P*	95% CI
Astra Tech OsseoSpeed	Prefabricated	0.79	0.36	0.004	.985	−0.46, 0.47	31.3	9.8	3.3	.622	−11.8, 18.4
	CAD/CAM	0.78	0.24				29.0	10.4			
Bränemark System	Prefabricated	0.61	0.27	0.33	.059	−0.67, 0.02	22.3	6.0	1.0	.755	−6.8, 8.9
	CAD/CAM	0.94	0.05				21.2	3.9			
NobelReplace	Prefabricated	1.37	0.24	0.02	.922	−0.38, 0.35	47.7	9.3	15.0	.026	−27.0, −2.9
	CAD/CAM	1.38	0.25				62.6	2.7			
Straumann Bone Level	Prefabricated	0.97	0.24	0.34	.213	−0.95, 0.27	28.0	1.2	1.1	.674	−7.8, 5.6
	CAD/CAM	1.31	0.47				29.1	5.3			
Straumann Standard Plus	Gold prefabricated	0.41	0.05	1.86	.002	−2.53, −1.19	14.2	3.1	34.4	< .001	−42.2, −26.6
	CAD/CAM	2.08	0.95	0.20	.701	−1.39, 1.00	4.0	1.2	44.7	< .001	−52.3, −37.0
		2.28	0.53				48.7	6.0			

SD = standard deviation; CI = confidence interval.

High magnification images of the implant-abutment connection were then taken using digital SEM (Quanta Model 200, FEI) under low vacuum and in an electron backscatter mode. Sixteen images at ×6,000 magnification were taken at equidistant intervals along each of the two key areas for all implant connection designs that were defined as the flange, representing the more horizontal load-bearing areas, and the vertical components, which are designed to assist with indexing and rotational resistance. The flange and vertical components for each of the implant types are depicted in Fig 1. Lower magnifications were used when the gap was larger than 50 µm, as it exceeded the field of view at ×6,000 magnification.

Because of their double hex configuration as depicted in Fig 2, samples BE (Branemark System/esthetic), AT (Astra Tech/TiDesign), and AP (Astra Tech/NobelProcera) were then further ground and polished, according to the above regime, to enable new SEM images to be taken for evaluation of the internal fit of the hexagon.

Pixel-counting software (Image J, National Institutes for Health) was then used to measure the implant-abutment microgap at eight equidistant points along each image. The measurements were compiled to produce a mean gap for the two connection areas of each specimen. Statistical analysis was performed with independent *t* tests (Minitab 16) to compare the mean gap values between the CAD/CAM and prefabricated abutments for each implant type.

Results

Representations of the data for each individual specimen are depicted in Figs 3 and 4, which indicate the variability of each specimen. Statistical comparisons between the fit of the CAD/CAM and prefabricated groups for the flange and vertical components on each of the implant systems are shown in Table 2.

Flange

The gold synOcta abutments were found to have a statistically smaller mean microgap by 1.86 µm (P = .002) on the implant flange when compared with the CAD/CAM abutments. The Nobel Esthetic abutments were also found to have a smaller mean microgap by 0.33 µm on the implant flange, which was close to statistical significance (P = .059), compared with the CAD/CAM abutments. No statistically significant differences were observed between the mean microgap values of the CAD/CAM and prefabricated abutments for the remainder of the groups.

Vertical

The CAD/CAM abutments were found to have greater mean vertical discrepancies by 15 µm compared with the Nobel Esthetic abutments for the NobelReplace implant system, which was statistically significant (P = .026). For the Straumann Standard Plus implant,

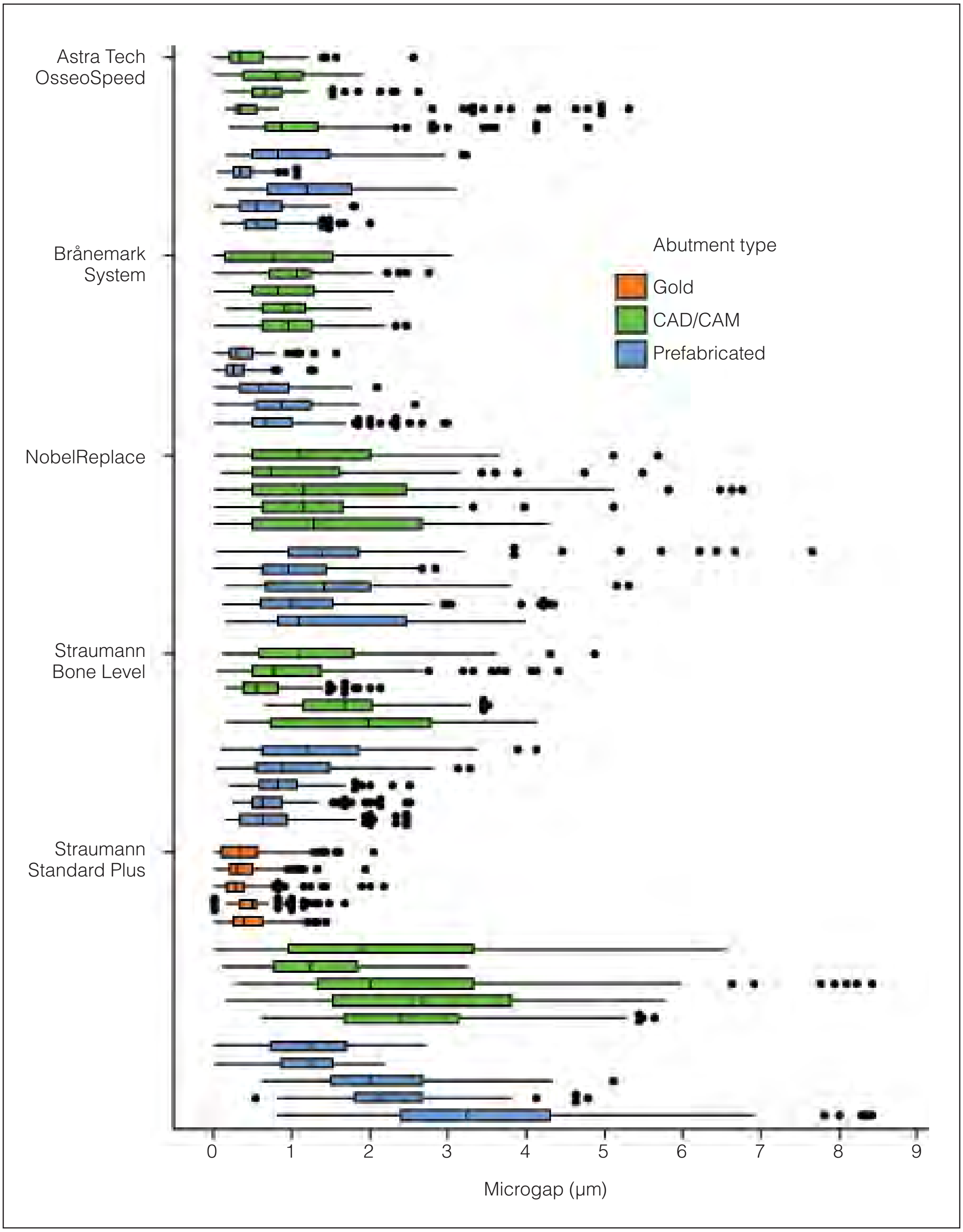

Fig 3 Flange data.

the CAD/CAM abutments were also found to have greater mean vertical discrepancies by 34.4 µm and 44.7 µm compared with the gold synOcta and titanium synOcta abutments, respectively (*P* < .001). No statistically significant differences were observed between the mean vertical gap values of the CAD/CAM and prefabricated abutments for the remainder of the groups. The prefabricated abutments were also observed to extend approximately 900 µm and 1,200 µm deeper into the connection when compared with the CAD/CAM abutments on the Straumann Standard Plus and the Straumann Bone Level implants, respectively.

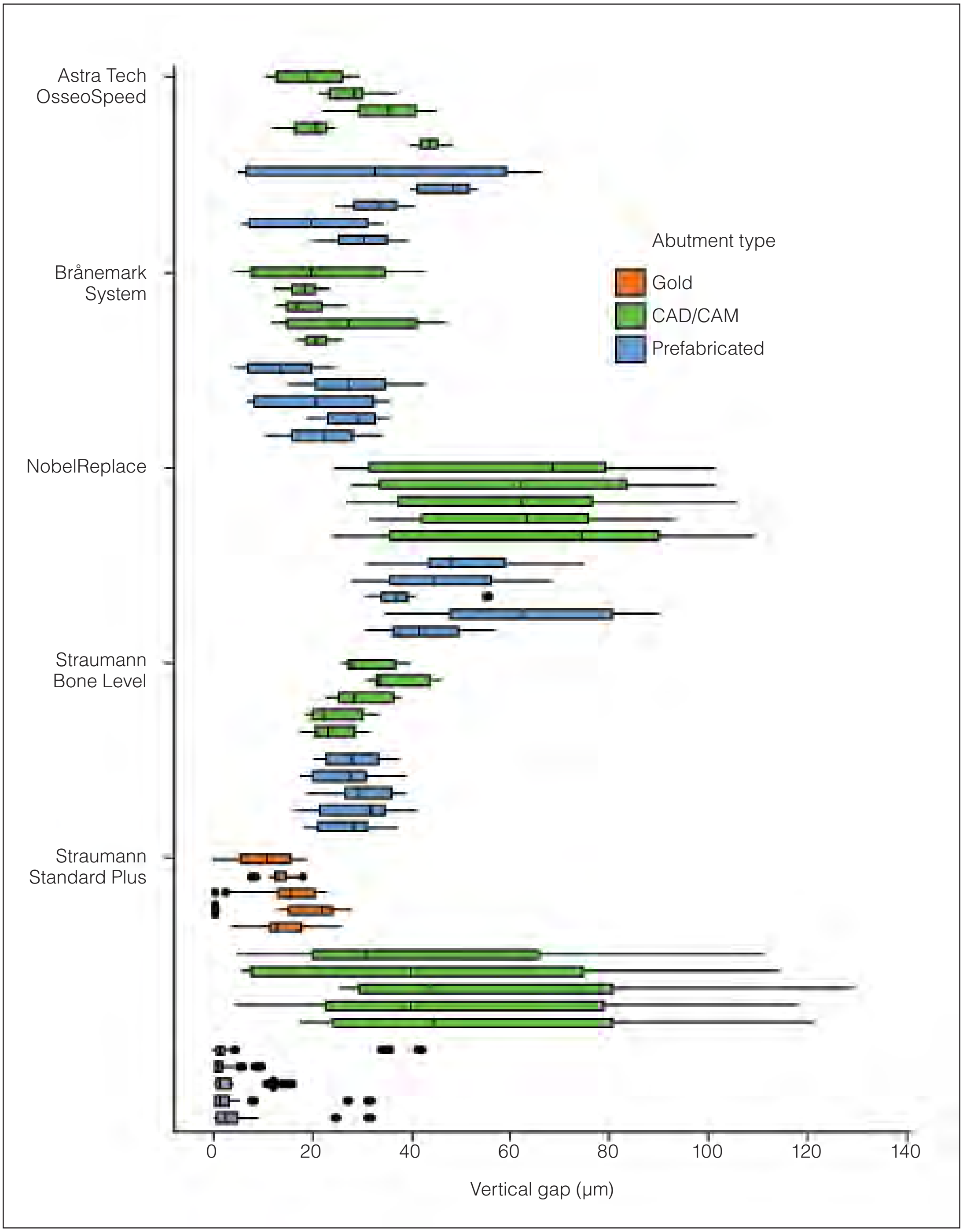

Fig 4 Vertical data.

SEM Observations

SEM images of the surfaces of the components prior to assembly demonstrated residual surface irregularity and characteristics that may be attributed to the machining processes. Grooves were visible on both the fitting surfaces of the implants and abutments that appeared to correspond with the path of the machining tools (Fig 5). The cross-sectional SEM images demonstrated contact between the implant and abutments only at the peaks of the grooves (Fig 6). The gold synOcta abutment appeared to have less irregularity on its fitting surface (Figs 5e and 5f) that was also visible as a flatter surface in the cross-sectional images (Fig 6a).

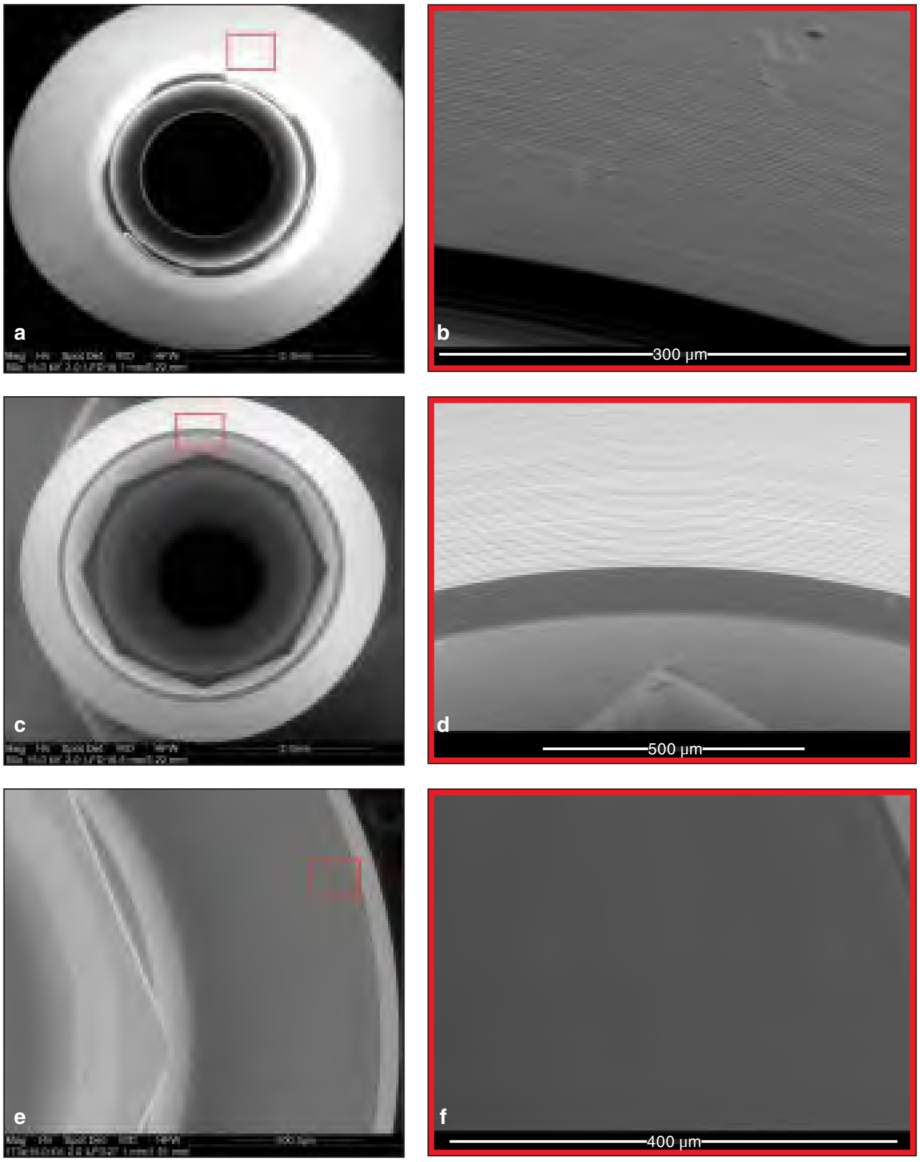

Fig 5 SEM images displaying concentric grooves formed on the mating surfaces during manufacturing for **(a and b)** Straumann RC Anatomic abutment and **(c and d)** Straumann Standard Plus implant. **(e and f)** A finer surface finish is visible on the mating surface of the Straumann synOcta gold abutment.

Discussion

The microgeometry of connecting parts has great importance in terms of proper function, prevention of premature failure, and ease of manufacture, assembly, and cost.[29] Some important microgeometric features include: *(1)* the design and specification of fit between mating parts to ensure proper function, *(2)* the specification of allowable variation in the manufactured part dimensions (tolerances) that will not compromise the specified fit, and *(3)* the specification of surface texture and condition that will ensure proper function, minimize failure potential, and optimize overall cost.[29–31] The combination of these three features will determine the amount of overall misfit present when two components are assembled.[32]

Mechanical means of sectioning and polishing of the implant-abutment specimens to enable direct visualization of the implant-abutment interface can produce significant deformation on the surface of the specimen.[33] Titanium is an inherently difficult material to polish and possesses a unique susceptibility to sustained mechanical deformation thought to be due to its low thermal conductivity and high ductility. This can result in the smearing of the materials and polishing residue into the spaces between the components. In this study, metallographic polishing techniques were used to provide a relatively deformation-free

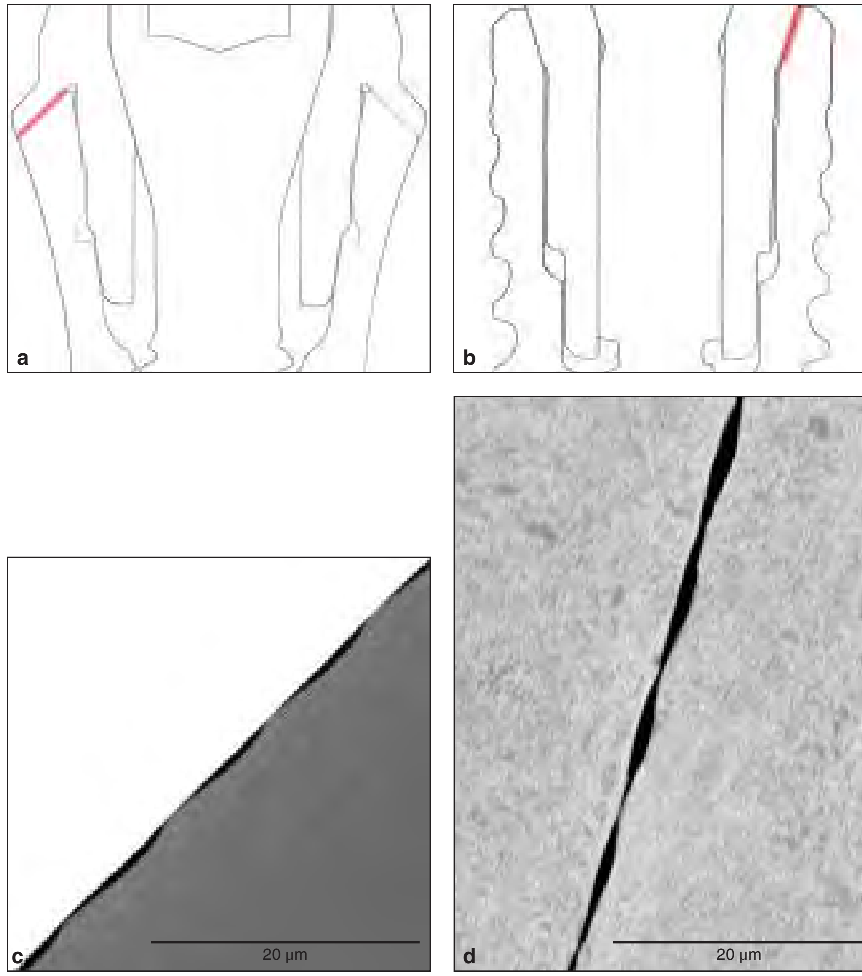

Fig 6 **(a and b)** Schematic diagrams of the Straumann Standard Plus and Straumann Bone Level implants indicating location of the cross-sectional SEM images of the mating surfaces between **(c)** Straumann Standard Plus implant and synOcta gold abutment. The gold abutment on the superior aspect appears white in the back scatter SEM mode due to its higher molecular weight. The profile of the grooves visible on the mating surface of the Straumann Standard Plus implant is clearly visible. **(d)** Straumann anatomical abutment *(left)* and a Straumann Bone Level implant *(right)* displaying contact between the peaks of the grooves on each of the mating surfaces.

surface that was able to be verified with visualization of the titanium grain structure under polarized light microscopy.[26–28,34,35] Such a deformation-free surface enables an accurate evaluation of any discontinuities or gaps between the components.

Previous studies have used coarser mechanical polishing following sectioning that does not produce a deformation-free surface.[36–40] This may explain why several authors have described various connections being completely sealed at the implant-abutment interface.[39] However, more recent synchrotron-based radiography supports the existence of a gap along the entire length of the implant-abutment interface of internal conical connections from 1 to 4 μm without loading and up to 22 μm under dynamic loading conditions.[14] Leakage of corpuscular bodies and molecular leakage from within the implant-abutment assemblies with all connection types has also been demonstrated under static[4–6,8,10] and dynamic loading conditions,[9] indicating that a complete seal is not present. This may lead to the ingress and egress of fluid during dynamic loading conditions.[15]

The reference points for measurements and the descriptive terminology defining fit vary considerably among investigators. An implant-abutment fit classification system has been proposed by Kano et al; however, this only encompasses the external marginal fit of the implant-abutment interface.[22] The

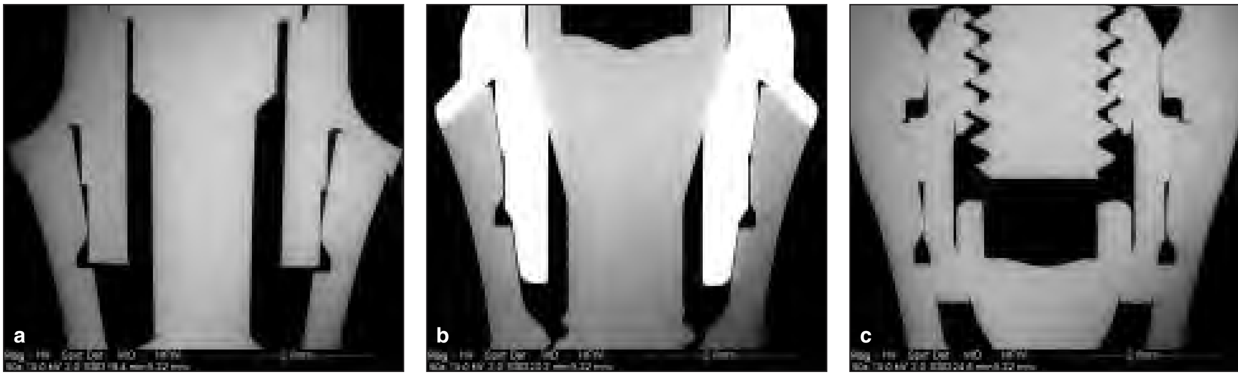

Fig 7 Cross-sectional images of **(a)** Procera, **(b)** gold synOcta, and **(c)** titanium synOcta abutment on the Straumann Standard Plus implant.

measurement of fit along the whole implant-abutment interface was chosen for this study as differences in the internal fit of the connection may significantly affect the biomechanical behavior of the implant-abutment interface.[38,41,42]

Two separate areas were assessed and compared for each of the connection designs: the implant flange (depicted in red, Fig 1) representing contacting load-bearing areas of the connection, and vertical components (depicted in green, Fig 1) thought to provide additional antirotational features and resistance to lateral loading and also used for prosthetic indexing. The fit was assessed as the approximation of the two components, with the size of the measured gap indicating the level of misfit. The mean gap size was used for statistical comparison to give an overall comparison of fit. The large variability of each of the individual specimens depicted in Figs 3 and 4 suggests that an assessment of more specific areas may have shown further differences in fit. The variability seen may have also been influenced by the machining tolerances and variations in the size of the components.

In this study, significant differences ($P < .001$) were found between the mean vertical gaps in the internal tapered section of the Straumann Standard Plus implants of the CAD/CAM abutments (48.7 ± 6.0 μm) and that of the prefabricated titanium (4 ± 1.2 μm) and gold (14.2 ± 3.1 μm) abutments. These differences are also evident in Fig 4, which displays the vertical data for each individual specimen and shows that the gaps ranged from 5 to 129 μm. This is due to internal design differences within the connection of the CAD/CAM abutments that do not engage the internal conical taper of the Straumann Standard Plus implant connection, resulting in a tapering wedge-shaped gap clearly visible in Fig 7a. The gold and titanium synOcta abutments appear to more closely follow the internal tapered design of the Straumann Standard Plus implant (Figs 7b and 7c).

A gold synOcta abutment was also used for comparison on the Straumann Standard Plus implant as there is no prefabricated one-piece titanium abutment that engages both the internal and external features of the implant connection. Although the gold synOcta followed the design of the internal taper, a consistent gap averaging 14.2 μm was present along its length with no areas of direct contact. The friction lock mechanism of the internal conical taper connection is thought to play a significant role in the antirotational resistance of the abutment that may help reduce screw loosening as well as stress transmission and resistance to lateral forces.[1,19,43,44] The degrees of misfit present in the internal aspect of the CAD/CAM and gold prefabricated abutments may negatively affect the abutments' resistance to lateral and rotational forces; however, the smaller misfit present on the implant flange for the gold synOcta abutment may compensate for this to some degree.

The smaller depth of engagement of the CAD/CAM abutment on the Straumann Standard Plus and Straumann Bone Level implants may also negatively influence the resistance of the abutment to lateral forces. Several studies have demonstrated movement and gap formation between the implant and abutment during nonaxial loading.[14,15,45] Hermann et al was the first to propose that the movement between the implant and abutment may be the prime etiologic factor in crestal bone loss around the implant-abutment connection and not the microgap itself.[12] A mechanical and biologic rationale for this was further developed by Zipprich et al and termed the "micropump effect."[15]

Varying degrees of irregularities, in the form of grooves, were observed on the fitting surfaces for all implant and abutment types. These grooves appear to be characteristic of the machining processes used during manufacturing of the components. This observation corresponded with the appearance of the cross-sectional images depicting contact only on the peaks of the grooves. This reduces the contacting surface area between the components, which may be of critical importance for connection designs that employ a friction fit, antirotational mechanism.[46,47]

The gold synOcta abutment appeared to have a much finer surface finish, which may explain the statistically significant smaller mean implant-abutment microgap of 0.41 μm in this group compared to 2.28 μm for the CAD/CAM abutments (P = .002). Rough surface finishes may correspond to a greater misfit and should be further evaluated.

To maintain clinical relevance, the respective manufacturer's abutment screws and recommended torques were used throughout the study. The abutment screws for the CAD/CAM and prefabricated abutments differed in macroscopic design, material, and surface coatings. This may have influenced the degree of embedment relaxation and also the fit determined between the implant and abutments, as it has been shown that different screw designs, materials, and surface coatings can produce measurable differences in preload forces following the application of the same tightening torque.[48–50]

Conclusion

The CAD/CAM abutments appeared to have a comparable fit on the implant flange to the titanium prefabricated abutments for all implant types evaluated. The prefabricated gold abutment had a better fit on the flange of the Straumann Standard Plus implant than the titanium CAD/CAM abutment. Significantly larger gaps were found between the internal components of the CAD/CAM abutments than the prefabricated abutments on the Straumann Standard Plus and NobelReplace implants. Design differences between the CAD/CAM and prefabricated abutment connections for both Straumann implants were observed, which affected the fit of internal components within the connections. The effect of these differences in connection design and fit in relation to the stability of the implant-abutment connection, as well as their technical and biologic implications, warrants further investigation. The CAD/CAM abutments used in this study were provided by a single manufacturer, and the findings cannot be extrapolated to other CAD/CAM systems.

Acknowledgments

This project was supported by a Melbourne Dental School Research Grant, University of Melbourne, Australia, International Team for Implantology (ITI) Research Grant (no. 754 2011), Switzerland, and an Australian Prosthodontic Society Research Grant. The authors thank Emily Szycman (Melbourne Dental School) and Roger Curtain (Bio 21 Institute) for SEM assistance and Ilya Zalizniak (Melbourne Dental School) and Donald McAuley (Struers) for specimen preparation assistance. The authors also thank Sandy Clarke (University of Melbourne) for statistical analysis and Drs Gerald Clausen and Anthony Dickinson for manuscript assistance. The authors reported no conflicts of interest related to this study.

References

1. Binon PP. The effect of implant/abutment hexagonal misfit on screw joint stability. Int J Prosthodont 1996;9:149–160.
2. Kano SC, Binon P, Bonfante G, Curtis DA. Effect of casting procedures on screw loosening in UCLA-type abutments. J Prosthodont 2006;15:77–81.
3. Assunção WG, Dos Santos PH, Delben JA, Gomes ÉA, Barão VAR, Tabata LF. Effect of misfit on preload maintenance of retention screws of implant-supported prostheses. J Mater Eng Perform 2009;18:935–938.
4. do Nascimento C, Barbosa RES, Issa JPM, Watanabe E, Ito IY, Albuquerque RF Jr. Bacterial leakage along the implant-abutment interface of premachined or cast components. Int J Oral Maxillofac Surg 2008;37:177–180.
5. do Nascimento C, Barbosa RES, Issa JPM, Watanabe E, Ito IY, De Albuquerque RF Jr. Use of checkerboard DNA-DNA hybridization to evaluate the internal contamination of dental implants and comparison of bacterial leakage with cast or premachined abutments. Clin Oral Implants Res 2009;20:571–577.
6. Gross M, Abramovich I, Weiss EI. Microleakage at the abutment-implant interface of osseointegrated implants: A comparative study. Int J Oral Maxillofac Implants 1999;14:94–100.
7. Harder S, Dimaczek B, Açil Y, Terheyden H, Freitag-Wolf S, Kern M. Molecular leakage at implant-abutment connection-in vitro investigation of tightness of internal conical implant-abutment connections against endotoxin penetration. Clin Oral Investig 2009;13:1–6.
8. Jansen VK, Conrads G, Richter EJ. Microbial leakage and marginal fit of the implant-abutment interface. Int J Oral Maxillofac Implants 1997;12:527–540.
9. Steinebrunner L, Wolfart S, Bößmann K, Kern M. In vitro evaluation of bacterial leakage along the implant-abutment interface of different implant systems. Int J Oral Maxillofac Implants 2005;20:875–881.
10. Dibart S, Warbington M, Ming FS, Skobe Z. In vitro evaluation of the implant-abutment bacterial seal: The locking taper system. Int J Oral Maxillofac Implants 2005;20:732–737.
11. Hecker D, Eckert S, Choi Y. Cyclic loading of implant-supported prostheses: Comparison of gaps at the prosthetic-abutment interface when cycled abutments are replaced with as-manufactured abutments. J Prosthet Dent 2006;95:26–32.
12. Hermann JS, Schoolfield JD, Schenk RK, Buser D, Cochran DL. Influence of the size of the microgap on crestal bone changes around titanium implants. A histometric evaluation of unloaded non-submerged implants in the canine mandible. J Periodontol 2001;72:1372–1383.

13. Weng D, Nagata MJH, Bell M, Bosco AF, De Melo LGN, Richter EJ. Influence of microgap location and configuration on the periimplant bone morphology in submerged implants. An experimental study in dogs. Clin Oral Implants Res 2008;19:1141–1147.
14. Rack A, Rack T, Stiller M, Riesemeier H, Zabler S, Nelson K. In vitro synchrotron-based radiography of micro-gap formation at the implant-abutment interface of two-piece dental implants. J Synchrotron Radiat 2010;17:289–294.
15. Zipprich H, Weigl P, Lange B, Laurer H-C. Micromovements at the implant-abutment interface: Measurement, causes, and consequences. Implantologie 2007;15:31–46.
16. Kapos T, Ashy LM, Gallucci G, Weber H, Wismeijer D. Computer-aided design and computer-assisted manufacturing in prosthetic implant dentistry. Int J Oral Maxillofac Implants 2009;24:110–117.
17. Jemt T, Rubenstein JE, Carlsson L, Lang BR. Measuring fit at the implant prosthodontic interface. J Prosthet Dent 1996;75:314–325.
18. Rangert BR, Sullivan RM, Jemt TM. Load factor control for implants in the posterior partially edentulous segment. Int J Oral Maxillofac Implants 1997;12:360–370.
19. Merz BR, Hunenbart S, Belser U. Mechanics of the implant-abutment connection: An 8-degree taper compared to a butt joint connection. Int J Oral Maxillofac Implants 2000;15:519–526.
20. Binon P. Evaluation of machining accuracy and consistency of selected implants, standard abutments, and laboratory analogs. Int J Prosthodont 1995;8:162–178.
21. Dellow AG, Driessen CH, Nel HJC. Scanning electron microscopy evaluation of the interfacial fit of interchanged components of four dental implant systems. Int J Prosthodont 1997;10:216–221.
22. Kano SC, Binon PP, Curtis DA. A classification system to measure the implant-abutment microgap. Int J Oral Maxillofac Implants 2007;22:879–885.
23. Lang LA, Sierraalta M, Hoffensperger M, Wang RF. Evaluation of the precision of fit between the Procera custom abutment and various implant system. Int J Oral Maxillofac Implants 2003;18:652–658.
24. Ma T, Nicholls JI, Rubenstein JE. Tolerance measurements of various implant components. Int J Oral Maxillofac Implants 1997;12:371–375.
25. Vigolo P, Fonzi F, Majzoub Z, Cordioli G. Evaluation of gold-machined UCLA-type abutments and CAD/CAM titanium abutments with hexagonal external connection and with internal connection. Int J Oral Maxillofac Implants 2008;23:247–252.
26. Samuels LE. Modifications required to manual preparation systems. In: Samuels LE (ed). Metallographic Polishing by Mechanical Methods. Materials Park: ASM International, 2003:265–296.
27. Taylor B. Metallographic preparation of titanium–Struers application notes. In: Struers. Denmark: Rosendahls Bogtryk, 2008.
28. Vander Voort GF. Titanium specimen preparation. Adv Mater Processes 2008;166:25–27.
29. Collins JA, Busby HR, Staab GH. Geometry determination. In: Collins JA, Busby HR, Staab GH (eds). Mechanical Design of Machine Elements and Machines. Hoboken: John Wiley & Sons, 2009:305–332.
30. Budynas RG, Budynas R, Nisbett K. Limits and fits. In: Budynas RG, Budynas R, Nisbett K (eds). Shigley's Mechanical Engineering Design. New York: McGraw-Hill, 2010:395–408.
31. Dornfeld D, Lee DE. Introduction to precision manufacturing. In: Dornfeld D, Lee DE (eds). Precision Manufacturing. New York: Springer, 2007:1–48.
32. Grous A. Fundamentals of dimensional and geometrical tolerances according to ISO, CSA (Canada) and ANSI (USA). In: Grous A (ed). Applied Metrology for Manufacturing Engineering. London: John Wiley & Sons, 2011:85–162.
33. Shaw M. Precision engineering. In: Crookall J, Shaw M, Suh N (eds). Metal Cutting Principles. New York: Oxford University, 2005:573–602.
34. Vander Voort GF. Metallographic preparation of titanium and its alloys. In: Gorynin IV, Ushkov SS (eds). Titanium '99, vol 2. St. Petersburg: CRISM, 2000.
35. Vander Voort GF. Specimen preparation for metallographic examination of medical devices. Adv Mater Process 2009;167:51.
36. Baixe S, Fauxpoint G, Arntz Y, Etienne O. Microgap between zirconia abutments and titanium implants. Int J Oral Maxillofac Implants 2010;25:455–460.
37. Byrne D, Houston F, Cleary R, Claffey N. The fit of cast and premachined implant abutments. J Prosthet Dent 1998;80:184–192.
38. Coelho A, Suzuki M, Dibart S, DA Silva N, Coelho P. Cross-sectional analysis of the implant-abutment interface. J Oral Rehabil 2007;34:508–516.
39. Sumi T, Braian M, Shimada A, et al. Characteristics of implant-CAD/CAM abutment connections of two different internal connection systems. J Oral Rehabil 2012;39:391–398.
40. Tsuge T, Hagiwara Y, Matsumura H. Marginal fit and micro-gaps of implant-abutment interface with internal anti-rotation configuration. Dent Mater J 2008;27:29–34.
41. Binon P, McHugh M. The effect of eliminating implant/abutment rotational misfit on screw joint stability. Int J Prosthodont 1996;9:511–519.
42. Sahin S, Cehreli MC, Yalcin E. The influence of functional forces on the biomechanics of implant-supported prostheses: A review. J Dent 2002;30:271–282.
43. Sutter F, Weber HP, Sorensen J, Belser U. The new restorative concept of the ITI dental implant system: Design and engineering. Int J Periodontics Restorative Dent 1993;13:409–409.
44. Bozkaya D, Müftü S. Mechanics of the tapered interference fit in dental implants. J Biomechanics 2003;36:1649–1658.
45. Gratton DG, Aquilino SA, Stanford CM. Micromotion and dynamic fatigue properties of the dental implant-abutment interface. J Prosthet Dent 2001;85:47–52.
46. Thornley RH, Elewa I. The static and dynamic stiffness of interference shrink-fitted joints. Int J Mach Tool Design Res 1988;28:141–155.
47. Ramachandran RV, Radhakrishnan V. Influence on surface finish on interference fits. Int J Prod Res 1974;12:705-719.
48. Martin WC, Woody RD, Miller BH, Miller AW. Implant abutment screw rotations and preloads for four different screw materials and surfaces. J Prosthet Dent 2001;86:24–32.
49. Park CI, Choe HC, Chung CH. Effects of surface coating on the screw loosening of dental abutment screws. Metals Mater Int 2004;10:549–553.
50. Stüker R, Teixeira E, Beck J, da Costa N. Preload and torque removal evaluation of three different abutment screws for single standing implant restorations. J Appl Oral Sci 2008;16:55–58.